Statistical Mechanics of 2-D Fluids

by

Nikhil Padhye, B.Tech.

Thesis

Presented to the Faculty of the Graduate School
of The University of Texas at Austin
in Partial Fulfillment
of the Requirements
for the Degree of

Master of Arts

The University of Texas at Austin
May, 1994

Statistical Mechanics of 2-D Fluids

APPROVED BY
SUPERVISING COMMITTEE:

Supervisor: Philip J. Morrison

Philip J. Morrison

Richard D. Hazeltine

Richard D. Hazeltine

Acknowledgements

I am grateful to my advisor, Phil Morrison, for his enthusiastic guidance and support. I also wish to thank him, Neil Balmforth and Richard Hazeltine for critically reading preliminary forms of this thesis and making helpful suggestions. I also enjoyed the opportunity to interact with Brad, Diego, Raul, John and Bill during the Friday afternoon meetings.

Nikhil Padhye
April, 18th, 1994.

ABSTRACT

Statistical Mechanics of 2-D Fluids

by

Nikhil Padhye, M.A.
The University of Texas at Austin, 1994
SUPERVISOR: Philip J. Morrison

Various approaches to study the turbulent relaxation of 2-D fluids are discussed. The results are compared to an experiment on electrons in a magnetized column.

Contents

Chapter 1

Introduction

Two dimensional fluid flows are realized in situations where one dimension is much smaller than the other two or if symmetry allows the neglect of one of the dimensions. Other factors, too, can contribute to result in effectively two dimensional (henceforth 2-D) flows. An example is the planetary atmospheric and oceanic flow where rotation of the fluid about the planet's axis locks it into 2-D motion (Taylor-Proudman theorem). See Greenspan (1968) for the dynamics of rotating fluids. A constant magnetic field perpendicular to a layer of plasma has a similar locking effect (Kraichnan and Montgomery, 1980) which is why there is some interest in 2-D magnetohydrodynamics. One of the interesting features of 2-D flows is the formation of coherent structures, an example of which is the Great Red Spot of Jupiter. An experiment by Sommeria, Meyers and Swinney (1988) demonstrated the formation of coherent structures in 2-D turbulent shear by creating a "Great Red Spot" in a rotating tank of fluid. The problem of 2-D flows is also interesting purely from the point of view of studying the dynamics, hence the wish to study 2-D fluid flows.

Various approaches to study the turbulent relaxation of 2-D flows are discussed in this thesis. We begin by setting up the basic equations and by reviewing the Hamiltonian formulation of the dynamics in Chapter 1. In

Chapter 2 we discuss statistical approaches to solve the problem of turbulent relaxation. These approaches include the point vortex approximation and the method of maximizing entropy. While the fluid is approximated by a collection of point vortices in the former case, the latter approach allows us to deal with continuous vorticity distributions, although, in practice, one discretizes the vorticity in order to compute the results numerically. Chapter 3 is devoted to the study of a selective decay hypothesis based on arguments of cascade of energy and enstrophy to different scales. After having discussed these three different approaches, we then compare their predictions to the observations in an experiment on electrons in a magnetized column in Chapter 4. The possibility of a simple monotonic restacking of the vorticity is also discussed in Chapter 4.

1.1 The 2-D Euler Equation for the Ideal Fluid

The Euler equation for an inviscid and incompressible fluid is

$$\frac{\partial \mathbf{v}}{\partial t} + \mathbf{v} \cdot \nabla \mathbf{v} = -\frac{\nabla P}{\rho} , \tag{1.1}$$

where $\mathbf{v}(\mathbf{r})$ is the fluid velocity at position $\mathbf{r}$, ρ is the density, assumed constant everywhere in the fluid, $P(\mathbf{r})$ is the pressure and it is assumed that there are no external forces acting on the fluid (Landau & Lifshitz, 1959). One can eliminate the pressure (and any external forces which can be written as the gradient of a potential) by taking the curl of eq. (1.1) to get

$$\frac{\partial \boldsymbol{\omega}}{\partial t} + \mathbf{v} \cdot \nabla \boldsymbol{\omega} = \boldsymbol{\omega} \cdot \nabla \mathbf{v} , \tag{1.2}$$

where $\boldsymbol{\omega} := \nabla \times v$ is the vorticity. This equation simplifies further in the case where the velocity is restricted to two dimensions, i.e. where one component of the velocity is constant and there is no variation of the two other components in that direction. For such two dimensional flows, the vorticity lies

entirely along the ignorable direction; thus the right hand side of eq. (1.2) is zero. Explicitly, the resulting vorticity equation is

$$\frac{\partial \omega}{\partial t} + \mathbf{v} \cdot \nabla \omega = 0 \,, \tag{1.3}$$

where ω is now the scalar vorticity defined by $\omega := \hat{\mathbf{z}} \cdot \nabla \times \mathbf{v}$ and we assume that the velocity has a $\hat{\mathbf{z}}$ component which is constant and variation is in the $\hat{\mathbf{x}}$ and $\hat{\mathbf{y}}$ directions only. Henceforth we restrict our attention to such 2-D flows.

For incompressible fluids,

$$\nabla \cdot \mathbf{v} = 0 \,, \tag{1.4}$$

which motivates us to define a streamfunction, ψ, such that

$$\mathbf{v} = \nabla \psi \times \hat{\mathbf{z}} \,, \tag{1.5}$$

thus ensuring a divergenceless velocity field. In terms of the streamfunction the scalar vorticity may now be expressed as

$$\omega = -\nabla^2 \psi \tag{1.6}$$

and the equation of motion (1.3) can now be written as

$$\frac{\partial \omega}{\partial t} = [\psi, \omega] \,, \tag{1.7}$$

where the square bracket is defined by

$$[f, g] := \frac{\partial f}{\partial x}\frac{\partial g}{\partial y} - \frac{\partial f}{\partial y}\frac{\partial g}{\partial x} \,. \tag{1.8}$$

Having expressed the equation of motion in the form of eq. (1.7), in the rest of this chapter we review the Hamiltonian formulation for this equation of motion.

1.2 Hamiltonian Description of the 2-D Ideal Fluid

The energy of the 2-D, inviscid fluid is purely kinetic. Thus one may write the Hamiltonian as

$$H[\mathbf{v}] = \frac{1}{2}\int_D v^2(\mathbf{r})\, d^2r \,, \tag{1.9}$$

where $H[\mathbf{v}]$ indicates that H is a functional of $\mathbf{v}$ and D is the domain, $\mathbf{r} = (x, y) \in D$. In terms of the streamfunction the Hamiltonian can be expressed as

$$H[\psi] = \frac{1}{2}\int_D |\nabla\psi|^2\, d^2r = \frac{1}{2}\int_D (\nabla\cdot(\psi\nabla\psi) - \psi\nabla^2\psi)\, d^2r \,. \tag{1.10}$$

The boundary condition is that the component of $\mathbf{v}$ normal to the boundary vanishes. This implies that $\nabla\psi$ is normal to the boundary, i.e. ψ is constant on the boundary. Hence the first term on the right-hand side of eq. (1.10) vanishes after integrating by parts. Then using eq. (1.6) the Hamiltonian can be written as

$$H[\omega] = \frac{1}{2}\int_D \omega\psi\, d^2r = \frac{1}{2}\int\int \omega(r)G(r,\tilde{r})\omega(\tilde{r})\, d^2r d^2\tilde{r} \,, \tag{1.11}$$

where $G(r, \tilde{r})$ is a Green's function which inverts eq. (1.6), i.e.

$$\psi(r) = \int_D G(r,\tilde{r})\omega(\tilde{r}) d^2\tilde{r} \,. \tag{1.12}$$

We now define the noncanonical Poisson bracket (Morrison, 1981) as

$$\{F, G\} := \int_D \omega \left[\frac{\delta F}{\delta\omega}, \frac{\delta G}{\delta\omega}\right] d^2r \,, \tag{1.13}$$

where $\delta F/\delta\omega$ is the functional derivative of F with respect to ω and the square bracket inside the integral is as defined earlier by eq. (1.8). For a Hamiltonian structure we require that the bracket be antisymmetric, that is

$$\{F, G\} = -\{G, F\} \,, \tag{1.14}$$

be linear in one of the arguments,

$$\{F, \alpha G + \beta H\} = \alpha\{F, G\} + \beta\{F, H\} \quad \text{for constants } \alpha \text{ and } \beta\,, \tag{1.15}$$

and satisfy the Jacobi identity:

$$\{\{F, G\}, H\} + \{\{G, H\}, F\} + \{\{H, F\}, G\} = 0\,. \tag{1.16}$$

Note that equations (1.14) and (1.15) together imply that the bracket is bilinear. For the bracket defined by eq. (1.13) antisymmetry follows from the fact that the square bracket is antisymmetric. Linearity follows from the linearity of the square bracket and of the integral operator. The Jacobi identity requires more work, but it can be shown that it is satisfied. For the meaning of noncanonical Hamiltonian structure and details of the Hamiltonian description of fluids see Morrison (1994). In the next section we obtain the equation of motion and constants of motion.

1.3 Constants of Motion

Upon integrating by parts and neglecting the boundary terms one can show that

$$\int_D f[g, h]\, d^2r = -\int_D g[f, h]\, d^2r\,, \tag{1.17}$$

for functions f, g and h defined on the domain, D, and assuming that the behavior of f, g and h allows the neglect of the boundary terms. Eq. (1.17) will be now be used to obtain both the equation of motion and the constants of motion. To obtain the equation of motion we note from equations (1.11) and (1.12) that

$$\frac{\delta H}{\delta \omega} = \psi \tag{1.18}$$

and thus see that

$$\frac{\partial \omega}{\partial t} = \{\omega, H\} = -\left[\omega, \frac{\delta H}{\delta \omega}\right] = [\psi, \omega]\,, \tag{1.19}$$

which is the same as eq. (1.7). In obtaining eq. (1.19) we have made use of both, eq. (1.17) and that

$$\frac{\delta\omega(r)}{\delta\omega(\tilde{r})} = \delta(r - \tilde{r}) \,. \tag{1.20}$$

Now suppose there exists a constant of motion, $C[\omega]$. Then its bracket with the Hamiltonian should vanish since

$$0 = \frac{\partial C}{\partial t} = \{C, H\} \,. \tag{1.21}$$

Making use of eq. (1.17) we see that this is satisfied if

$$\left[\omega, \frac{\delta C}{\delta \omega}\right] = 0 \,, \tag{1.22}$$

which is true if $\delta C/\delta\omega$ is any function of ω. In fact, then the bracket of C with any functional of ω vanishes. In particular, its bracket with the Hamiltonian vanishes which makes it a constant of the motion. Such constants of motion originate in the structure of the bracket (the kinematics), rather than the dynamics and are called "Casimirs". For the 2-D Euler equation we have the Casimirs expressed by

$$C[\omega] = \int_D \mathcal{C}(\omega)\, d^2r \,, \tag{1.23}$$

where $\mathcal{C}(\omega)$ is an arbitrary function of the vorticity, ω.

Chapter 2

Statistical Methods

The nonlinearity in the Euler equation makes it impossible to solve analytically in a general case. The study of the dynamics using numerical techniques is also awkward since one requires finer and finer grids as time increases. One way to approach the problem is to explore a statistical technique to find the state to which the fluid might relax, if any. In this chapter we study two such statistical techniques which have been developed. The first approach, Point Vortex Approximation, approximates the vorticity distribution by a collection of point vortices and exploits the resulting finite degree-of-freedom canonical Hamiltonian system. The second approach, Maximum Entropy Flows, allows a continuous vorticity distribution and conserves all the Casimirs.

2.1 Point Vortex Approximation

A finite degree-of-freedom, canonical Hamiltonian description of the 2-D fluid can be obtained when the vorticity field is approximated by a collection of moving point vortices:

$$\omega(\mathbf{r}) = \sum_{i=1}^{n} \omega_i \, \delta(\mathbf{r} - \mathbf{r}_i) \, , \tag{2.1}$$

where $\mathbf{r}_i(t)$ is the position of the ith vortex which has circulation ω_i and ω obtains its dependence on time through the $\mathbf{r}_i$'s. We now follow Morrison (1981) to obtain the canonical Hamiltonian description for this system of discrete vortices starting with the noncanonical Poisson bracket defined by eq. (1.13).

When ω depends on an independent variable, μ, in addition to $\mathbf{r}$ then one has

$$\frac{\partial F}{\partial \mu} = \int_D \frac{\delta F}{\delta \omega} \frac{\partial \omega}{\partial \mu} d^2 r \ , \tag{2.2}$$

where F is considered to be some function of μ on the left and as a functional of ω on the right. Using eq. (2.1) in the above equation and integrating by parts gives

$$\frac{\partial F}{\partial x_j} = \omega_j \frac{\partial}{\partial x} \frac{\delta F}{\delta \omega}(x_j, y_j) \tag{2.3}$$

and similarly for the y_js where we are now using $\mathbf{r} = (x, y)$. Making use of equations (2.1) and (2.3) in (1.13) allows us to write the bracket as

$$\{F, G\} = \sum_{i=1}^{n} \frac{1}{\omega_i} \left(\frac{\partial F}{\partial x_i} \frac{\partial G}{\partial y_i} - \frac{\partial F}{\partial y_i} \frac{\partial G}{\partial x_i} \right) \ , \tag{2.4}$$

which is a canonical Poisson bracket, with coordinates $\omega_i x_i$ and y_i canonically conjugate to each other. Thus the phase space coincides with the configuration space. The equations of motion are given by

$$\frac{dx_i}{dt} = \{x_i, H\} = \frac{1}{\omega_i} \frac{\partial H}{\partial y_i} \ ; \ \frac{dy_i}{dt} = \{y_i, H\} = -\frac{1}{\omega_i} \frac{\partial H}{\partial x_i} \ . \tag{2.5}$$

Using eq(2.1) in (1.11) shows that the Hamiltonian may be expressed as

$$H = \frac{1}{2} \sum_{i,j=1; i \neq j}^{n} \omega_i \omega_j G(r_{ij}) \ , \tag{2.6}$$

where $r_{ij} = \sqrt{(x_i - x_j)^2 + (y_i - y_j)^2}$. If the domain is the real plane (infinite domain) then the Green's function has the form

$$G(r_{ij}) = -\frac{1}{2\pi} \log r_{ij} \ .$$

For a finite domain one can express the energy in terms of a sum over the log r_{ij}'s but then, just as in electrostatics, one has to include image terms arising from the boundary as well. Instead we choose to express the energy in terms of the Green's function. Note that we avoid the singularity when $i = j$, that is, we subtract the infinite self-energy of the vortices.

Before proceeding to use statistical mechanics to calculate the distribution for a specific case, we present an argument due to Onsager (1949) which points out a peculiarity of the statistical mechanics for this system which arises due to the finiteness of phase space. The phase space element is $d\zeta \equiv dx_1 dy_1 \cdots dx_n dy_n$ and the phase volume which corresponds to energies less than a given value, E, is defined to be

$$\Phi(E) := \int_{H<E} d\zeta =: \int_{-\infty}^{E} \Phi'(E)\, dE \,,$$

where $\Phi'(E)$ is the structure function. The energy, E, takes all values from $-\infty$ to $+\infty$ and clearly we have

$$\Phi(-\infty) = 0 \quad ; \quad \Phi(+\infty) = A^n \,,$$

where A is the area of the domain. Also, it must be true that $\Phi'(E)$ is positive for all E. This, together with the finite value of the integral over all energies, implies that $\Phi'(E)$ must assume its maximum value for some finite, critical value of energy, E_c. Hence

$$\Phi''(E_c) = 0 \,;$$

$\Phi''(E)$ is positive for $E < E_c$ and negative for $E > E_c$. Note that it is possible to have more than one maximum, in which case there are more than one energy-intervals which correspond to negative temperatures. Assuming equal a priori probability of occupying the available phase space for a given energy we use the usual definition of the entropy and temperature for a microcanonical ensemble:

$$S := k \log \Phi' \quad ; \quad \frac{1}{T} \equiv \frac{\partial S}{\partial E} = \frac{1}{k} \frac{\Phi'}{\Phi''} \,.$$

Thus we see that

$$T > 0 \text{ for } E < E_c \;\; ; \;\; T < 0 \text{ for } E > E_c \, .$$

Note that it is possible to have more than one maximum of Φ', in which case there are more than one energy-intervals which correspond to negative temperatures. The possibility of having negative temperatures gives rise to some interesting behavior. Negative temperatures correspond to high energy configurations which, in turn, correspond to clusters of vortices of the same sign. Thus we see that such clusters are a possible outcome of this approach. This matches well, qualitatively, with observations of small scale eddies combining to form long lived regions of vorticity in 2-D turbulence (Sommeria, Meyers and Swinney, 1988). It is also borne out by numerical simulations of the dynamics (Marcus, 1988).

We now calculate vorticity distribution in the canonical ensemble when, in addition to energy, the angular momentum is conserved, i.e. we consider an axisymmetric system. Furthermore, the system is a collection of point vortices all of which have the same sign. (We shall later discuss an experiment to which this calculation applies.) Montgomery and Joyce (1974) showed that one can make use of the Gibb's measure even in the negative temperature regime. Thus we have

$$\begin{aligned} < \omega(x,y) > \;\; = \;\; & \frac{1}{Z} \int \left\{ \left[\sum_{i=1}^{n} \omega_i \, \delta(x - x_i) \, \delta(y - y_i) \right] \exp \left[-\beta (\sum_{j>k=1}^{n} \omega_j \omega_k G_{jk}) \right] \right. \\ & \left. \exp \left[-\frac{\gamma}{2} (\sum_{l=1}^{n} \omega_l (R^2 - r_l^2)) \right] \right\} \prod_{m=1}^{n} dx_m dy_m, \end{aligned} \tag{2.7}$$

where β and γ arise as Lagrange multipliers for the energy and the angular momentum respectively, $G_{ij} := G(r_{ij})$, $r_i^2 := x_i^2 + y_i^2$ and Z is the partition function defined by

$$Z = \int exp \left[-\beta (\sum_{j>k=1}^{n} \omega_j \omega_k G_{jk}) - \frac{\gamma}{2} (\sum_{l=1}^{n} \omega_l (R^2 - r_l^2)) \right] \prod_{m=1}^{n} dx_m \, dy_m \, . \tag{2.8}$$

Note that the angular momentum, $\int \mathbf{r} \times \mathbf{v}\, d^2r$, can be written as $\int \omega(R^2 - r^2)/2\, d^2r$ after integrating by parts. Then using the expression for the vorticity, eq. (2.1), one gets the sum as shown in the integrals above. The expression for the distribution of the vorticity can then be reduced to the following:

$$< \omega >= \sum_{i=1}^{n} C_i \omega_i \, exp[-\beta \omega_i \psi - \frac{\gamma}{2} \omega_i (R^2 - r^2)] \,, \tag{2.9}$$

where C_i's are constants which can be determined once one knows β and γ and the Green's function. Eq. (2.9), alongwith $\nabla^2 \psi = - < \omega >$ allows us to solve for $\psi(x, y)$. The Green's function depends on the boundary conditions for the particular domain while β and γ can be determined from the initial energy and angular momentum. Usually one assumes that all the point vortices are of the same strength in order to simplify matters.

Having illustrated the point vortex approach by means of the preceding example we now proceed to study another statistical approach. More examples and details of calculations involving the point vortex approximation may be found in Smith (1991) and Edwards & Taylor (1974).

2.2 Maximum Entropy Flows

The maximum entropy approach involves coarse graining and preserves all the invariants of motion. It was first proposed by Lynden-Bell (1967) in the context of violent relaxation of star clusters and has been rediscovered independently by others in recent years (Miller, 1990; Robert and Sommeria, 1991).

We assume that the vorticity takes on discrete values but is piecewise continuous initially. Thus $\omega \in (\omega_1, \omega_2, \cdots, \omega_n)$. The vorticity equation (1.3) may also be expressed as

$$\frac{d\omega}{dt} = 0 \,, \tag{2.10}$$

where the derivative is the total (or Lagrangian) derivative, which means that

in a frame which moves with a fluid element there is no change in the vorticity. This makes it clear that the effect of the dynamics is to relocate the vorticity. We assume that some time later the boundaries of the constant vorticity regions are intricately spread over the domain. The spatial fluctuation of vorticity is very rapid, but on small enough scales we still have piecewise continuous vorticity. Thus we have two scales - the piecewise continuous vorticity on small scales and the mean flow on a larger scale. We define a "cell" on the larger scale to consist of a large number, N, of "subcells". We also define P_i to be the total number of subcells with vorticity ω_i and $M_{\mu i}$ to be the number of subcells, with vorticity ω_i, present in the μ^{th} cell. (Note that the Greek subscript labels the cell while the Latin subscript labels the value of vorticity.) Evidently, P and M are related by

$$P_i = \sum_{\mu} M_{\mu i} \, .$$

Lynden-Bell (1967) now counts the number of ways, W_L, of distributing the subcells among the cells as:

$$W_L = \left\{ \prod_i \frac{P_i!}{\prod_\mu M_{\mu i}!} \right\} \left\{ \prod_\mu \frac{N!}{(N - \sum_i M_{\mu i})!} \right\} \, . \tag{2.11}$$

The first part in the above formula represents the number of ways in which P_i subcells can be distributed into groups of M_{1i}, M_{2i}, etc. The second part represents the distribution within a single cell. $(N - \sum_i M_{\mu i})$ are the number of "empty" subcells in the μ^{th} cell. Thus the counting, within a cell, considers the subcells (particles) as being distinguishable (irrespective of whether or not they possess the same value of the vorticity) and only one subcell can occupy a site; there can only be N subcells in a cell. In this sense the statistics may be thought of as being like Maxwell-Boltzmann counting in considering distinguishable particles, yet resembling Fermi-Dirac statistics in the sense that there is an exclusion principle. However, it is interesting to note that the first part of the distribution (i.e. P_i subcells distributed into groups of

M_{1i}, M_{2i}, etc.) considers the subcells to be indistinguishable. Also note that within a cell the empty subcells are considered indistinguishable.

Empty cells made sense in the stellar context in which the statistics were derived, but in the fluid context there are no empty subcells. Alternatively, Miller (1990) and Robert and Sommeria (1991) count the number of states as follows:

$$W = \prod_{\mu} \left\{ \frac{N!}{\prod_i M_{\mu i}!} \right\} . \tag{2.12}$$

This counting is easier to interprete. The part inside the curly bracket is the number of ways of distributing the subcells within a cell. Here, in contrast to Lynden-Bell's counting, we consider subcells with the same value of vorticity to be indistinguishable. Then one takes the product of the distributions over each of the cells to get the total number of ways to distribute the subcells.

Inspite of the difference in interpretation, the two ways of counting are, in fact, identical. This can be seen by setting $(N - \sum_i M_{\mu i})$ either equal to zero or including it as being one of the $M_{\mu i}$'s in eq. (2.11) and by interchanging the product over μ and i. Then one has the result

$$W = \frac{W_L}{\prod_i P_i!} , \tag{2.13}$$

i.e. the two ways of counting are related simply by a constant which depends on the initial conditions.

We now define the entropy of the μ^{th} cell to be

$$\frac{1}{N} \log W_\mu ,$$

where

$$W_\mu = \frac{N!}{\prod_i M_{\mu i}} . \tag{2.14}$$

Then, assuming N is large, we can use Stirling's formula to write

$$\frac{1}{N} \log W_\mu = -\sum_i p_i \log p_i , \tag{2.15}$$

where the probability, p_i, of finding vorticity, ω_i, in the μ^{th} macrocell is defined by

$$p_i(\mu) \equiv \frac{M_{\mu i}}{N} .$$

Now we take the limit as the size of the subcells and of the cells goes to zero, but such that there always are N subcells in a cell. Then the cell may be labelled by the position, $\mathbf{r}$, and the product over μ in eq. (2.12) is transformed into an integral over the domain to get the total entropy,

$$S[p] = -\int_D \sum_i p_i(\mathbf{r}) \log p_i(\mathbf{r})\, d^2r . \tag{2.16}$$

Our goal, now, is to maximize the entropy subject to the constraints of constant energy and Casimirs. The energy may be expressed as

$$H[p] = \frac{1}{2}\int_D \psi \,(\sum_i \omega_i p_i)\, d^2r , \tag{2.17}$$

where ψ, as earlier, is the streamfunction, which is assumed to be smooth although the vorticity is not. (This is plausible since the vorticity is the Laplacian of the streamfunction.) The conservation of the Casimirs is equivalent to the conservation of the areas of each of the vorticity patches (Morrison, 1987; Robert and Sommeria, 1991). This may be expressed as

$$A_i[p_i] \equiv \int_D p_i(\mathbf{r})\, d^2r = constant,\ i = 1, 2, \cdots, n . \tag{2.18}$$

In the limit that the vorticity distribution is continuous, there are an infinite number of constraints. These correspond to the infinite number of Casimirs of the form shown in eq. (1.23). Crudely, one may see that the conditions, eq. (2.18) and eq. (1.23), are equivalent by thinking of eq. (2.18) as saying that ω as well as d^2r are constant for a fluid element. That would then imply that the integral of an arbitrary function of ω is conserved. Another constraint, that of probability conservation, is

$$\sum_i p_i(\mathbf{r}) = 1 \ \ \forall \mathbf{r} \in D . \tag{2.19}$$

For an axisymmetric system we have another constraint, that of conservation of angular momentum. For a region of radius R, we may write the angular momentum as

$$L = \frac{1}{2}\int_0^R (\sum_i \omega_i p_i)(R^2 - r^2)\, 2\pi r\, dr\ , \tag{2.20}$$

just as was defined in the previous section, except that we have now replaced the vorticity by its local average. This is justified because $(R^2 - r^2)$ is smooth. Variation of $(S - \gamma L - \beta H - \sum_i \alpha_i A_i)$ with respect to p_i gives

$$\frac{\delta S}{\delta p_i} - \gamma \frac{\delta L}{\delta p_i} - \beta \frac{\delta H}{\delta p_i} - \alpha_i \frac{\delta A_i}{\delta p_i} = 0 \tag{2.21}$$

as the condition for an extremum, where γ, β and α_i's are Lagrange multipliers. Using equations (2.16), (2.17), (2.18) and (2.20) in eq. (2.21) we get the result

$$p_i = \frac{1}{Z} \exp[-\alpha_i - \beta\omega_i\psi - \gamma\omega_i(R^2 - r^2)/2]\ , \tag{2.22}$$

with the partition function, Z, given by

$$Z = \sum_i \exp[-\alpha_i - \beta\omega_i\psi - \gamma\omega_i(R^2 - r^2)/2]\ ; \tag{2.23}$$

p_i and Z obtain their dependence on $\mathbf{r}$ through ψ in addition to the Gaussian dependence on r. The solution is not complete until we find $\psi(\mathbf{r})$ for the relaxed state. This can be accomplished by solving the equation

$$-\nabla^2\psi = \sum_i \omega_i p_i = -\frac{1}{\beta}\frac{d\, log\, Z(\psi)}{d\psi}\ . \tag{2.24}$$

The Lagrange multipliers, α_i's, β and γ, are found from the initial conditions using the constraints stated in equations (2.17) and (2.18) and (2.20).

Although the above results appear very similar to the results in the previous section, of the point vortex approximation, note that the point vortex approximation does not have any α_i's in it, which arose in this (maximum entropy) approach due to the conservation of the Casimirs. In the continuum limit, $\alpha_i \to \alpha(\omega)$, thus conserving an infinite number of Casimirs.

Chapter 3

The Selective Decay Hypothesis

In this chapter we consider the effect of viscosity on 2-D fluid dynamics. It is shown, from the structure of the noncanonical Poisson bracket in eq. (1.13), that on Fourier decomposing the vorticity and truncating the system to neglect high k-values, only one out of the infinite number of Casimirs survives as a constant of motion, in general. We indicate why this particular Casimir, the enstrophy, might selectively dissipate more than the energy and present the resulting principle of minimizing enstrophy at constant energy to obtain the equilibrium flow.

3.1 Effects of Viscosity and Truncation

On modifying eq. (1.3) to allow viscosity we get

$$\frac{\partial \omega}{\partial t} + \mathbf{v} \cdot \nabla \omega = \nu \nabla^2 \omega \, . \tag{3.1}$$

Multiplying the above equation by ω and integrating we get an expression for the rate of change of the enstrophy:

$$\frac{d\Omega}{dt} = -\nu \int_D |\nabla \omega|^2 d^2 r \, , \tag{3.2}$$

where the enstrophy, Ω, is a Casimir which is defined to be

$$\Omega = \frac{1}{2}\int_D \omega^2 \, d^2r \, . \tag{3.3}$$

To obtain eq. (3.2) we used the incompressibility condition and assumed that the boundary condition is either periodic over the domain or that the perpendicular component of the velocity vanishes at the boundary. From eq. (3.2) it is clear that the enstrophy definitely decreases on introducing viscosity. Similarly it is seen for the energy that

$$\frac{dH}{dt} = -\nu \int_D \omega^2 \, d^2r = -2\nu\Omega \, . \tag{3.4}$$

We see that the energy is conserved in the absence of viscosity but decreases otherwise. In the Fourier transformed space, equations (3.2) and (3.4) may be written as:

$$\frac{d\Omega}{dt} = -\nu \sum_{\mathbf{k}} k^2 \omega_{\mathbf{k}}^2 \; ; \; \frac{dH}{dt} = -\nu \sum_{\mathbf{k}} \omega_{\mathbf{k}}^2 \, , \tag{3.5}$$

where we have Fourier decomposed the vorticity as

$$\omega(\mathbf{r}) = \sum_{\mathbf{k}} \omega_{\mathbf{k}} e^{i\mathbf{k}\cdot\mathbf{r}} \, , \tag{3.6}$$

with

$$\omega_{\mathbf{k}} = \frac{1}{(2\pi)^2}\int_D \omega(\mathbf{r}) e^{-i\mathbf{k}\cdot\mathbf{r}} \, d^2r \, . \tag{3.7}$$

Periodic boundary conditions are assumed and the summation in eq. (3.6) is an infinite summation, ranging over all $\mathbf{k}$ values.

From eq. (3.5) it is seen that the enstrophy decays much more rapidly at the high k-values than the energy. This is the basis of the selective decay hypothesis which we shall discuss in section 3.3. In this section, we now proceed to find the implications of a truncation of the Fourier modes on the constants of motion. The reason for contemplating such a truncation of the Fourier modes is the strong effect of viscosity at the high k-values that we

expect from eq. (3.1). A couple of other reasons why one might wish to truncate the modes are mentioned in the concluding section.

The energy may be expressed in terms of the Fourier modes of the vorticity as:

$$H = 2\pi^2 \sum_{\mathbf{k}} \frac{|\omega_{\mathbf{k}}|^2}{k^2} \,. \tag{3.8}$$

Neglecting the factor of $2\pi^2$, we may write

$$\frac{dH}{dt} = \sum_{\mathbf{k}} \frac{1}{k^2} \{\omega_{\mathbf{k}} \frac{d\omega_{\mathbf{k}}^*}{dt} + c.c.\} \,, \tag{3.9}$$

where the star indicates complex conjugation. We shall show below that

$$\Theta := \sum_{\mathbf{k}} \frac{\omega_{\mathbf{k}}}{k^2} \frac{d\omega_{\mathbf{k}}^*}{dt}$$

is zero. The same argument can also be applied to the complex conjugate term. Since the energy is real, we have

$$\omega_{\mathbf{k}}^* = \omega_{-\mathbf{k}} \,. \tag{3.10}$$

To obtain the equations of motion we observe that functional derivatives with respect to the vorticity can be expressed as a sum of terms involving derivatives with respect to the $\omega_{\mathbf{k}}$'s as:

$$\frac{\delta F}{\delta \omega} = \sum_{\mathbf{k}} \frac{\partial F}{\partial \omega_{\mathbf{k}}} \frac{\delta \omega_{\mathbf{k}}}{\delta \omega} = \frac{1}{(2\pi)^2} \sum_{\mathbf{k}} \frac{\partial F}{\partial \omega_{\mathbf{k}}} e^{-i\mathbf{k}\cdot\mathbf{r}} \,. \tag{3.11}$$

Thus the Poisson bracket for the 2-D Euler equation can be expressed as:

$$\{F, G\} = \frac{1}{(2\pi)^2} \sum_{\mathbf{k},\ell} \frac{\partial F}{\partial \omega_{\mathbf{k}}} \omega_{\mathbf{k}+\ell} \, \hat{\mathbf{z}} \cdot (\ell \times \mathbf{k}) \frac{\partial G}{\partial \omega_{\ell}} \,. \tag{3.12}$$

Hence the equations of motion in terms of the Fourier modes are

$$\frac{d\omega_{\mathbf{k}}}{dt} = \{\omega_{\mathbf{k}}, H\} = \sum_{\ell} \frac{\hat{\mathbf{z}} \cdot (\mathbf{k} \times \ell)}{\ell^2} \omega_{\ell} \, \omega_{\mathbf{k}-\ell} \,. \tag{3.13}$$

Thus we get

$$\Theta = \sum_{\mathbf{k}} \frac{\omega_{\mathbf{k}}}{k^2} \sum_{\ell} \frac{\hat{\mathbf{z}} \cdot (-\mathbf{k} \times \ell)}{\ell^2} \omega_{\ell}\, \omega_{-\mathbf{k}-\ell} = \sum_{\mathbf{k},\ell} \frac{\hat{\mathbf{z}} \cdot (\ell \times \mathbf{k})}{k^2 \ell^2} \omega_{\mathbf{k}}\, \omega_{\ell}\, \omega_{-\mathbf{k}-\ell} \,. \quad (3.14)$$

It is clear that the expression which is being summed on the right-hand side of eq. (3.14) is antisymmetric under interchange of $\mathbf{k}$ and ℓ (due to the vector product) and hence the sum is zero irrespective of the range over which the indices run. The energy is thus seen to be invariant for a truncated system.

We now turn our attention to the enstrophy in a truncated system. From the structure of the bracket in eq. (3.12) it is seen that a Casimir, C, must satisfy

$$\sum_{\ell} \omega_{\mathbf{k}+\ell}\, \hat{\mathbf{z}} \cdot (\ell \times \mathbf{k}) \frac{\partial C}{\partial \omega_{\ell}} = 0 \quad \text{for all } \mathbf{k} \,, \quad (3.15)$$

so that its bracket with an arbitrary function of the Fourier modes vanishes. We now specify the Casimir as being the enstrophy, Ω, given by

$$\Omega = 2\pi^2 \sum_{\mathbf{k}} |\omega_{\mathbf{k}}|^2 \,. \quad (3.16)$$

Then, neglecting numerical factors, we note that

$$\frac{\partial \Omega}{\partial \omega_{\ell}} = \omega_{-\ell} \,,$$

whereby the left-hand side of eq. (3.15) may now be expressed as

$$\Phi := \sum_{\ell=-\Lambda}^{\Lambda} \hat{\mathbf{z}} \cdot (\ell \times \mathbf{k})\, \omega_{\mathbf{k}+\ell}\, \omega_{-\ell} \,. \quad (3.17)$$

In the above equation, we have allowed for the possibility of truncation by introducing $\Lambda := (\xi, \eta)$ as a limit on the summation. ξ and η are the limits in the two different directions and we allow all modes between $-\Lambda$ and $+\Lambda$. Now changing the label in eq. (3.17) from ℓ to $-\ell$ we get

$$\Phi = \sum_{\ell=-\Lambda}^{\Lambda} -\hat{\mathbf{z}} \cdot (\ell \times \mathbf{k})\, \omega_{\mathbf{k}-\ell}\, \omega_{\ell} \,. \quad (3.18)$$

We transform eq. (3.17), again, in a different manner: we change the label from $\mathbf{l}$ to $\tilde{\mathbf{l}} := \mathbf{l} + \mathbf{k}$ and get

$$\Phi = \sum_{\tilde{l}=-\Lambda+\mathbf{k}}^{\Lambda+\mathbf{k}} \hat{\mathbf{z}} \cdot (\tilde{\ell} \times \mathbf{k}) \omega_{\mathbf{k}-\tilde{l}} \omega_{\tilde{l}} \,. \tag{3.19}$$

In the complete system (i.e. non-truncated) $\xi, \eta \to \infty$ and it is clear that the right-hand sides of equations (3.18) and (3.19) have opposite signs, hence $\Phi = 0$. However, for the truncated case it might seem at first that the ranges of summation are different and hence Φ might not be zero. But on closer inspection one notices that the same terms contribute to the sum in either case. For example, if $\mathbf{k}$ is positive (i.e. both of its components are positive) then the effective range for either summation is from $\mathbf{k} - \mathbf{\Lambda}$ to $\mathbf{\Lambda}$. This is because all other modes are zero due to the truncation. Hence the enstrophy is invariant in a truncated system.

We now adopt a different approach which enables us to see the effect of truncation more generally on all the Casimirs. A function, $f(\mathbf{r})$, may be expressed in terms of a Fourier series as

$$f(\mathbf{r}) = \sum_{\mathbf{k}} f_{\mathbf{k}} e^{i\mathbf{k}\cdot\mathbf{r}} \,, \tag{3.20}$$

where

$$f_{\mathbf{k}} = \frac{1}{(2\pi)^2} \int_D f(\mathbf{r})\, e^{-i\mathbf{k}\cdot\mathbf{r}}\, d^2r \,. \tag{3.21}$$

To see the effect of a truncation in $\mathbf{k}$ space on $f(\mathbf{r})$ we use eq. (3.21) in eq. (3.20) to get

$$\tilde{f}(\mathbf{r}) = \frac{1}{(2\pi)^2} \int_D d^2r'\, f(\mathbf{r}') \sum_{\mathbf{k}} e^{i\mathbf{k}\cdot(\mathbf{r}'-\mathbf{r})} \,. \tag{3.22}$$

If the summation over $\mathbf{k}$ in eq. (3.22) is infinite then

$$\sum_{\mathbf{k}} e^{i\mathbf{k}\cdot(\mathbf{r}'-\mathbf{r})} = (2\pi)^2\, \delta(\mathbf{r}' - \mathbf{r}) \tag{3.23}$$

and one recovers $\tilde{f}(\mathbf{r}) = f(\mathbf{r})$ as expected. However, for a truncated system, assuming the box is large, one might approximate the sum by an integral as

$$\sum_{\mathbf{k}=-\Lambda}^{\Lambda} e^{i\mathbf{k}\cdot(\mathbf{r}'-\mathbf{r})} \approx \int_{-\Lambda}^{\Lambda} e^{i\mathbf{k}\cdot(\mathbf{r}'-\mathbf{r})}\, d^2k = \int_{-\infty}^{\infty} e^{i\mathbf{k}\cdot(\mathbf{r}'-\mathbf{r})}\, W(k_x, k_y)\, d^2k \ , \quad (3.24)$$

where $W(k_x, k_y)$ is defined to be a window:

$$W(k_x, k_y) = \begin{cases} 1 & \text{if } |k_x| < \xi \text{ and } |k_y| < \eta \\ 0 & \text{elsewhere.} \end{cases}$$

Using the well known Fourier transform of the window, one gets the result

$$\tilde{f}(\mathbf{r}) = \frac{1}{\pi^2} \int_D d^2r'\, f(\mathbf{r}') \frac{\sin \xi(x'-x)}{(x'-x)} \frac{\sin \eta(y'-y)}{(y'-y)} \ . \quad (3.25)$$

Thus the process of truncation in the transformed space has its equivalent in the untransformed space of operating on $f(\mathbf{r})$ by the integral operator as shown above to get $\tilde{f}(\mathbf{r})$. It is no surprise that $\tilde{f}(\mathbf{r}) \neq f(\mathbf{r})$ in general.

We now recall the condition for the Casimir, eq. (1.22), which is restated here:

$$\left[\omega, \frac{\delta C}{\delta \omega}\right] = 0 \ . \quad (3.26)$$

This condition is satisfied if

$$\frac{\delta C}{\delta \omega} = g(\omega) \ ,$$

where $g(\omega)$ is an arbitrary function of the vorticity, ω, and depends on $\mathbf{r}$ through ω. On setting $f(\mathbf{r}) = \omega(\mathbf{r})$ in eq. (3.25) we see how ω transforms under truncation and call it $\tilde{\omega}$. Similarly, g changes to $\tilde{g}$. Now, in the truncated system we require that a Casimir, $\tilde{C}[\tilde{\omega}]$, satisfy

$$\left[\tilde{\omega}, \frac{\delta \tilde{C}}{\delta \tilde{\omega}}\right] = 0 \ , \quad (3.27)$$

which implies that $\delta\tilde{C}/\delta\tilde{\omega}$ be an arbitrary function of $\tilde{\omega}$. Moreover, if the Casimir is to survive the truncation, i.e. $\tilde{C} = C$, then $\delta\tilde{C}/\delta\tilde{\omega}$ must be the same function, g. However, in general,

$$\tilde{g}(\omega) \neq g(\tilde{\omega}) \, .$$

An obvious exception is if $g(\omega) = \omega$ (or some multiple of ω). This is precisely why enstrophy survives the truncation while the other Casimirs do not. (Note that the enstrophy, Ω, has $\delta\Omega/\delta\omega = \omega$.) Actually, some of the other Casimirs that we had for the non-truncated system can possibly survive the truncation, but from eq. (3.25) one sees that these would have to depend on the particular truncation. Also, one has new Casimirs for the truncated system (arbitrary functions of $\tilde{\omega}$) but these too depend on the particular truncation due to the dependence of $\tilde{\omega}$ on the particular truncation. It must also be noted that we retained all the modes below a certain cutoff in obtaining eq. (3.25). Other truncation schemes are also possible. Hald (1976) gives some interesting examples of constants of motion that survive certain truncation schemes. On the other hand, it is clear that the invariance of the enstrophy does not depend on any particular truncation and hence we call it a "rugged" invariant.

Thus we can infer the ruggedness of the enstrophy from eq. (3.26), which, in turn, stems from the structure of the Poisson bracket in eq. (1.13) and the property mentioned in eq. (1.17).

3.2 Energy and Enstrophy Spectra

In the preceding section we have seen that the energy and the enstrophy are rugged invariants. We now construct a statistical argument using these two invariants and obtain their equilibrium spectra. From eq. (3.13) it is seen that

$$\frac{\partial\dot{\omega}_{\mathbf{k}}}{\partial\omega_{\mathbf{k}}} = 0 \, , \tag{3.28}$$

where the dot indicates differentiation with respect to time. Hence, Liouville's theorem, which is

$$\sum_{\mathbf{k}} \frac{\partial \dot{\omega}_{\mathbf{k}}}{\partial \omega_{\mathbf{k}}} = 0 \,, \tag{3.29}$$

is satisfied. In fact, eq. (3.28) is stronger than eq. (3.29) since it shows that each phase space coordinate is volume preserving independently of the others and is sometimes referred to as the detailed Liouville theorem. The advantage in having the detailed Liouville theorem satisfied is that one can truncate the modes and yet have a volume preserving phase space. However, it should be noted that a truncation upsets the Hamiltonian structure and the bracket defined by eq. (3.12) no longer satisfies the Jacobi identity.

We now define the statistical average of a quantity, g, which is a function of the $\omega_{\mathbf{k}}$'s, as:

$$< g >:= \frac{1}{Z} \int \prod_{\mathbf{k}} d\omega_{\mathbf{k}}\, g \, \exp(-\beta H - \alpha \Omega) \,, \tag{3.30}$$

where the partition function, Z, is defined to be

$$Z := \int \prod_{\mathbf{k}} d\omega_{\mathbf{k}} \, \exp(-\beta H - \alpha \Omega) \,. \tag{3.31}$$

The average defined above may be thought of as an average over an ensemble of systems differing in energy and enstrophy, i.e. systems immersed in baths of energy and enstrophy. α may be thought of as the reciprocal "enstrophy temperature" and β as the (usual) reciprocal "energy temperature". With this definition of the average, one finds the average enstrophy associated with the $\mathbf{k}^{th}$ mode to be

$$< \Omega_{\mathbf{k}} >= 2\pi^2 < |\omega_{\mathbf{k}}|^2 >= \frac{k^2}{(\beta + \alpha k^2)} \tag{3.32}$$

and the average energy in the $\mathbf{k}^{th}$ mode is

$$< H_{\mathbf{k}} >= \frac{1}{(\beta + \alpha k^2)} \,. \tag{3.33}$$

Notice that β can be negative as long as $(\beta + \alpha k^2)$ is positive. (If $(\beta + \alpha k^2)$ is positive for the smallest value of k then it is positive for all k.) Thus, once again, negative energy-temperatures are allowed. Notice, also, that the enstrophy is uniformly distributed if β is zero while the energy is uniformly distributed if α is zero.

Equation (3.13) shows that the modes are coupled. This suggests that there is a flow of energy and enstrophy between modes. Fjortoft (1953) investigated the energy transfer in a triad (three modes) and concluded that if there is a transfer of energy out of the central mode then it must be transferred into both of the outer modes. The conservation of energy and enstrophy can be simultaneously satisfied only by a transfer of energy to higher as well as lower k's. One can infer the dominant direction of energy and enstrophy transfer from the statistical result obtained above. Assume that most of the energy and enstrophy is concentrated in the k^{th} mode to begin with. Then after a certain relaxation time the energy and enstrophy spectra take the form obtained above. The energy that has flowed to the $(2k)^{th}$ mode is then

$$\frac{1}{(\beta + 4\alpha k^2)},$$

while

$$\frac{1}{(\beta + \alpha \frac{k^2}{4})}$$

has flowed to the $(k/2)^{th}$ mode. If β is zero then it is clear that sixteen times as much energy has cascaded to the $(k/2)^{th}$ mode as compared to the $(2k)^{th}$ mode. Irrespective of the value of β, more energy flows to the lower k values than higher. A similar argument for the enstrophy shows that it cascades to higher values of k when β is positive and to lower k-values for negative β. Thus, again, we note the tendency to form large scale structures at negative temperatures. For positive temperatures, the energy flows to the larger length scales while the enstrophy flows to the smaller scales. (The scaling laws for such cascades are discussed by Kraichnan & Montgomery,

1980.)

Note that in the limit that k becomes infinite, $< \Omega_k >$ takes the value $1/\alpha$. The total enstrophy, which is $\sum_{\mathbf{k}} \Omega_{\mathbf{k}}$, is infinite unless a truncation is made.

3.3 Minimum Enstrophy Flows

We have noted in the preceding section that the energy cascades to larger length scales while the enstrophy cascades to the smaller scales where it is removed by the action of viscosity. Based on this cascade argument, Bretherton and Haidvogel (1976) suggested that 2-D flow should be that one with minimum enstrophy for a given energy. Thus we assume a selective decay, i.e. out of two key integrals, one decays appreciably more than the other. (This may also be argued from eq. (3.5).) A similar argument was used by Taylor (1974) in plasma physics, where he considers the magnetic helicity to be constant while the magnetic energy is minimized. Hasegawa (1985) interpretes such principles as exhibiting self-organization in one (the stronger) invariant and disorder in the other.

Minimum enstrophy flows are best illustrated by giving an example of the calculation. Since we will be discussing an experiment with cylindrical symmetry in the next section, we choose to calculate accordingly. The calculation follows on the lines of Leith (1984).

We assume that the vorticity is contained within a radius R and is zero outside it. Furthermore we set the radial velocity to be zero. The cylindrical symmetry implies that the total angular momentum is conserved. We also treat the energy and the total vorticity as being conserved. So, in fact, we are treating the energy, angular momentum and the total vorticity as rugged invariants while the enstrophy decays to a minimum. Introducing the variable

$$s := \frac{r}{R} ,$$

we express the velocity and the vorticity as follows:

$$v_\theta(r) := u(r/R) = u(s)$$

$$\omega(r) = \frac{1}{r}\frac{d(rv_\theta)}{dr} = \frac{1}{R}\frac{1}{s}\frac{d[su(s)]}{ds} =: \frac{W(s)}{R}$$

Thus we may now express the energy as

$$H = \frac{1}{2}\int_D v_\theta^2\, d^2r = \pi R^2 \int_0^1 u^2(s)\, s\, ds \tag{3.34}$$

and the total angular momentum as

$$L = \int_D r\, v_\theta\, d^2r = 2\pi R^3 \int_0^1 u(s)\, s^2\, ds\ . \tag{3.35}$$

The enstrophy can be written as

$$\Omega = \frac{1}{2}\int_D \omega^2\, d^2r = \pi \int_0^1 W^2(s)\, s\, ds \tag{3.36}$$

and, finally, the total vorticity can be written as

$$V = \int_D \omega\, d^2r = 2\pi R\, u(1)\ . \tag{3.37}$$

The variational principle is stated as

$$\delta\Omega - \alpha\delta V - \beta\delta H - \gamma\delta L = 0\ , \tag{3.38}$$

where α, β and γ are Lagrange multipliers. Variations are to be taken with respect to u and R and we require that $u(0) = 0$ and $u(1) = V/2\pi R$ which implies $\delta u(0) = 0$ and $\delta u(1) = 0$. Thus,

$$-2\pi \int_0^1 \delta u(s)\, \{\frac{dW}{ds} + \beta R^2 u(s) + \gamma R^3 s\}\, s\, ds\ - \frac{\delta R}{R}\{\alpha V + 2\beta H + 3\gamma L\} = 0\ . \tag{3.39}$$

Since this must be true for any δu and any δR we get the following conditions:

$$\alpha V + 2\beta H + 3\gamma L = 0 \tag{3.40}$$

and

$$\frac{dW}{ds} + \beta R^2 u(s) + \gamma R^3 s = 0 \,. \tag{3.41}$$

Multiplying eq. (3.41) by s and then differentiating with respect to s gives us

$$\frac{d^2W}{ds^2} + \frac{1}{s}\frac{dW}{ds} + a^2(W + \frac{2c}{a^2}) = 0;, \tag{3.42}$$

where $a^2 \equiv \beta R^2$, which implies that we seek $\beta > 0$, and $c \equiv \gamma R^3$. The solution to the vorticity distribution is therefore given by

$$W(s) = J_0(as) - \frac{2c}{a^2} \,, \tag{3.43}$$

where J_0 is the zeroth order Bessel function and the velocity profile is

$$u(s) = aJ_1(as) - cs \,, \tag{3.44}$$

where J_1 is the first order Bessel function. Using the above expressions in the formula for the energy gives

$$H = \frac{\pi R^2}{4}\left\{2a^2 J_1^2(a)\left[1 - \frac{2}{a}\frac{J_2(a)}{J_1(a)} + \frac{J_2^2(a)}{J_1^2(a)}\right] + c^2 - 8cJ_2(a)\right\} \,, \tag{3.45}$$

while the angular momentum is now

$$L = \frac{\pi R^3}{2}[4J_2(a) - c] \tag{3.46}$$

and the total vorticity is

$$V = 2\pi R[aJ_1(a) - c] \,. \tag{3.47}$$

If we know the initial energy, angular momentum and the total vorticity then we can figure out the three unknowns, a, c and R, from equations (3.45), (3.46) and (3.47). The Lagrange multipliers, β and γ, follow from a, c and R and then α can be found using eq. (3.40). The minimized enstrophy can be found from eq. (3.36).

Chapter 4

Experimental Results

Having discussed various approaches which predict the state to which the 2-D turbulent fluid relaxes – point vortex approximation, maximum entropy flows and minimum enstrophy flows – we now compare them to the observations in a recent experiment on a non-neutral plasma. We discuss the possibility of a simple monotonic restacking of the vorticity and also consider the possibility that some functional of the vorticity, other than enstrophy, might be the one that is selectively extremized.

4.1 An Experiment on Electrons in a Magnetized Column

Magnetized electron columns provide a good opportunity to study 2-D turbulence since the dissipation is low and the diagnostics are accurate. The $\mathbf{E} \times \mathbf{B}$ guiding center drift in the (r, θ) plane is described by the drift-Poisson equations:

$$\frac{\partial n}{\partial t} + \mathbf{v} \cdot \nabla n = 0 \tag{4.1}$$

$$\mathbf{v} = -\frac{c}{B} \nabla \phi \times \hat{\mathbf{z}} \tag{4.2}$$

$$\nabla^2 \phi = 4\pi e n \tag{4.3}$$

where $\mathbf{v}(r,\theta)$ is the drift velocity, B is the axial magnetic field perpendicular to the (r,θ) plane, $n(r,\theta)$ is the density of electrons, $\phi(r,\theta)$ is the electrostatic potential and $-e$ is the charge on an electron. The analogy between the magnetized electron column dynamics and 2-D fluid flows is seen by comparing the above equations to equations (1.3), (1.5) and (1.6). The transformation

$$\phi = -\frac{B}{c}\psi, \quad n = \frac{B}{4\pi ec}\omega$$

makes equations (4.1), (4.2) and (4.3) identical to equations (1.3), (1.5) and (1.6). Thus the electron density corresponds to the vorticity in fluids and the electrostatic potential corresponds to the streamfunction.

See Huang and Driscoll (1994) for the experimental details. In brief the experiment may be described as follows: Electrons are trapped in a cylindrical region with an axial magnetic field and externally applied electric field at the two ends. Measurements of the density profile are made by dumping the electrons onto an endplate. Since the measurement is destructive, the experiment has to be repeated many times; measurement is made at different time intervals after the electrons are trapped during the different runs. The initial density profile is hollow, azimuthally symmetric and is very nearly the same for each run. It is then found that the column quickly relaxes to a low noise metastable state which is maintained for some time and is then destroyed by collisions. The relaxation to the metastable state is, however, almost collisionless (Dubin & O'Neil, 1987).

On comparing the density profile of the metastable state to the predictions of the approaches of maximizing entropy, minimizing enstrophy and the point vortex approximation, Huang and Driscoll (1994) find that minimizing enstrophy predicts best. We shall discuss the pros and cons of the three techniques in the concluding section and indicate why minimizing enstrophy seems to be a better technique than the other two.

4.2 Entropy Production and Restacking

At this point we take the opportunity to point out a subtlety in defining the entropy in an experimental situation. Huang and Driscoll (1994) define the entropy as

$$S := -\int_D \frac{\omega}{\omega_0} \log \frac{\omega}{\omega_0} d^2r \,, \tag{4.4}$$

where ω_0 is a normalizing constant. Based on the above definition it is found that the entropy more than doubles in going from the initial to the metastable state. However, it can be shown that the definition, eq. (4.4), is ambiguous when the total vorticity is not conserved. To see that we rewrite eq. (4.4) as

$$\omega_0 S = \log \omega_0 \int_D \omega \, d^2r - \int_D \omega \log \omega \, d^2r \,. \tag{4.5}$$

Then the difference between the final and the initial entropy can be written as

$$\delta S = \frac{1}{\omega_0}(\delta V \log \omega_0 + \delta \mathcal{S}) \,, \tag{4.6}$$

where the total vorticity is defined by

$$V := \int_D \omega \, d^2r$$

and the quantity $\mathcal{S}$ is defined by

$$\mathcal{S} := -\int_D \omega \log \omega \, d^2r \,.$$

Thus it is seen from eq. (4.6) that for a non-zero δV, however small, the difference in entropies can take any value merely by adjusting ω_0. In particular, an ω_0 can be chosen which makes the difference vanish. And since there is no natural value of ω_0, the definition, eq. (4.4), is meaningless. In the experiment there was a small loss of electrons (total vorticity), i.e. δV was not zero, thus making eq. (4.4) inapplicable anyway.

Ideally, the entropy as defined by eq. (4.4) is a Casimir since it is a function of the vorticity alone and hence we expect it to be conserved; in the

absence of collisions there can be no increase in the entropy. One way to ensure that all the Casimirs, including entropy, are conserved is to monotonically restack the vorticity in r^2, as explained next.

We define the free energy, $F[\omega]$, (Morrison, 1987) by

$$F = H + C\,,$$

where C is a Casimir defined by eq. (1.23). Considering equilibria to be the stationary points of the free energy, we have a condition for equilibria,

$$\frac{\delta F}{\delta \omega} = 0 = \frac{\delta H}{\delta \omega} + \frac{\delta C}{\delta \omega} = \psi + \frac{\partial \mathcal{C}}{\partial \omega}\,. \tag{4.7}$$

In order to obtain a solution for $\omega(\psi)$, $\partial \mathcal{C}/\partial \omega$ must be monotonic, which implies that its inverse is monotonic too. Thus we seek $\omega(\psi)$ which is a monotonic function of ψ. Upon taking the second variation of F, we find that it is positive definite if

$$\frac{\partial^2 \mathcal{C}}{\partial \omega^2} > 0 \;\Rightarrow\; \frac{\partial \omega}{\partial \psi} = -\left[\frac{\partial^2 \mathcal{C}}{\partial \omega^2}\right]^{-1} < 0\,,$$

i.e. ω is a monotonically decreasing function of ψ. Thus a monotonically decreasing $\omega(\psi)$ which satisfies eq. (4.7) is a stable equilibrium.

In case of the 2-D fluid, we have seen earlier that the vorticity simply gets relocated. Hence one might wish to simply rearrange or "restack" the vorticity so that it is a monotonic function of the streamfunction. But the equilibrium streamfunction, itself, is an unknown. However, the geometry of the experiment comes to our rescue and suggests that the restacking should be carried out in r^2, i.e. the initial vorticity be plotted as a function of r^2 and then rearranged to make it a monotonically decreasing function of r^2. This is so that $\omega\, d^2r = \omega\, d(r^2)$ is conserved on each element, thus conserving the infinite number of Casimirs (Gardner, 1963). (Note that the solution is unique; there is only one way to rearrange a function in a monotonically decreasing fashion.) This also implies that we expect the equilibrium streamfunction to

behave as r^2. We carried out a couple of restackings using the initial data of Huang and Driscoll (1994). The restacking was carried out once in r^2 and once in the experimentally found equilibrium streamfunction. The results of both restackings were in excellent agreement. Not surprisingly, it was also found that the experimental equilibrium streamfunction behaved as r^2 in the critical region; the critical region being one in which restacking occurred. (Note that a portion of the vorticity does not undergo any restacking; it is already stacked.) The results are shown in figure (4.1) and are not very far off from the experimental results. Again, note that there is no change in entropy or in any other Casimir due to restacking.

However, the major drawback of the restacking argument is that although it is a minimum of the free energy, F, the energy, H, actually increases. In this case the energy increased by about 8 percent. Hence we conclude that the monotonic restacking is not accessible unless there is some energy input from the boundary. The fact that we see a monotonic vorticity distribution in the experiment suggests that all the Casimirs are not being conserved and the losses are important.

4.3 Conclusion

Onsager (1949) suggested the use of statistical mechanics to deal with the problem of 2-D turbulence. This first approach, which was based on approximating the vorticity field by a collection of point vortices, gives rise to a finite degree-of-freedom, canonical Hamiltonian description of the dynamics. Although this model gives good qualitative agreement with the observations of formation of coherent structures in turbulent shear flow, it suffers from the drawback of approximating a continuous vorticity field by point vortices; there is no unique way to accomplish it.

The maximum entropy approach of Lynden-Bell and others is conceptually more pleasing than the point vortex approach since it allows one to

consider a continuous vorticity field and conserves all the (infinite) Casimir invariants. In practice, one performs the numerical computation after discretizing the continuous vorticity distribution and conserves as many Casimir invariants as the number of discrete bits that are considered. Despite conserving the Casimirs this method does not seem to predict the experimental outcome as well as the selective decay hypothesis does. This indicates that the Casimirs are not being conserved as well as the ideal dynamics suggests and that the non-ideal effects at large k-values are quite important. Another possibility is that our assumption of ergodic mixing is far from the truth.

The large k region is definitely a delicate region which poses problems. Firstly, in any experiment there is bound to be some finite spatial resolution, d. This has the implication that in the measurement of any "initial" vorticity one has no information about modes with $k > 1/d$. So one hopes that these modes, if they exist, do not contribute much to the dynamics of the observable lower modes. In fact, from the equation of motion, it cannot altogether be ruled out that sufficiently strong high k modes will not affect the behavior of the low k modes. And since one bases one's calculations on such data, truncation cannot be much worse. Secondly, there is a scale length below which viscous effects are important. This may be estimated as $\sqrt{\nu\omega_{max}}$. Thirdly, there is the scale length, approximately the molecular size, below which the fluid approximation breaks down and discrete particle effects gain importance. Also, at these small scales one cannot really consider 2-D motion any longer, one must consider 3-D motion. Due to all these reasons one is not really interested in the exact solution to the 2-D Euler equation if one wants to explain observations. (The mode coupling of the 2-D Euler equation does not allow solutions with no contribution from the high k modes.)

The success of the selective decay hypothesis is probably because it treats the high k region differently from the low k region. As we have seen in chapter 3, truncation leads, generally, to the loss of all the constants of motion except energy and enstrophy. This is the key feature of the selective

decay hypothesis. On the other hand, truncation is clearly artificial and one loses some information. The truncated modes could have had some influence on the modes which have been retained and vice versa. What is the best way to truncate? Perhaps one should carry out many truncation schemes and find the average behavior or find the cutoffs for which a small change in the cutoffs makes no difference to the dynamics. Another drawback of the selective decay scheme is that it does not satisfactorily explain the choice of the invariants which are to be considered rugged. For example, in the calculation that was carried out in Chapter 3, it was assumed that the energy, total angular momentum and the total vorticity were rugged invariants while enstrophy was not.

When they hypothesised the minimum enstrophy flows, Bretherton and Haidvogel (1976) also discussed the possibility that some other functional of the vorticity might actually be the one extremized instead of the enstrophy. Using data from the experiment on magnetized electrons, we calculated, a posteriori, the Casimir which was extremized for that flow. That is, we found the function, $\mathcal{C}(\omega)$, which satisfies eq. (4.7). The result is shown in figure (4.2). The lowest order polynomial that fits $\mathcal{C}(\omega)$ is quadratic. This corresponds to the Casimirs used in the minimization of enstrophy – total vorticity and enstrophy – and is not entirely surprising since according to Huang and Driscoll's calculation the minimum enstrophy method did fit the data closely.

The selective decay hypothesis has been used in a variety of situations with some success. However, the experiment described in this Chapter probably has the most accurate diagnostics and more such experiments with a wide variety of initial conditions are required before one can be sure that the selective decay hypothesis is the key to the problem of 2-D turbulence.

Figure 4.1
The vorticity, monotonically restacked in r^2, is plotted against s (=r / R). The final experimental vorticity is also plotted for comparision. Data from Huang & Driscoll (1994) has been used in our calculation.

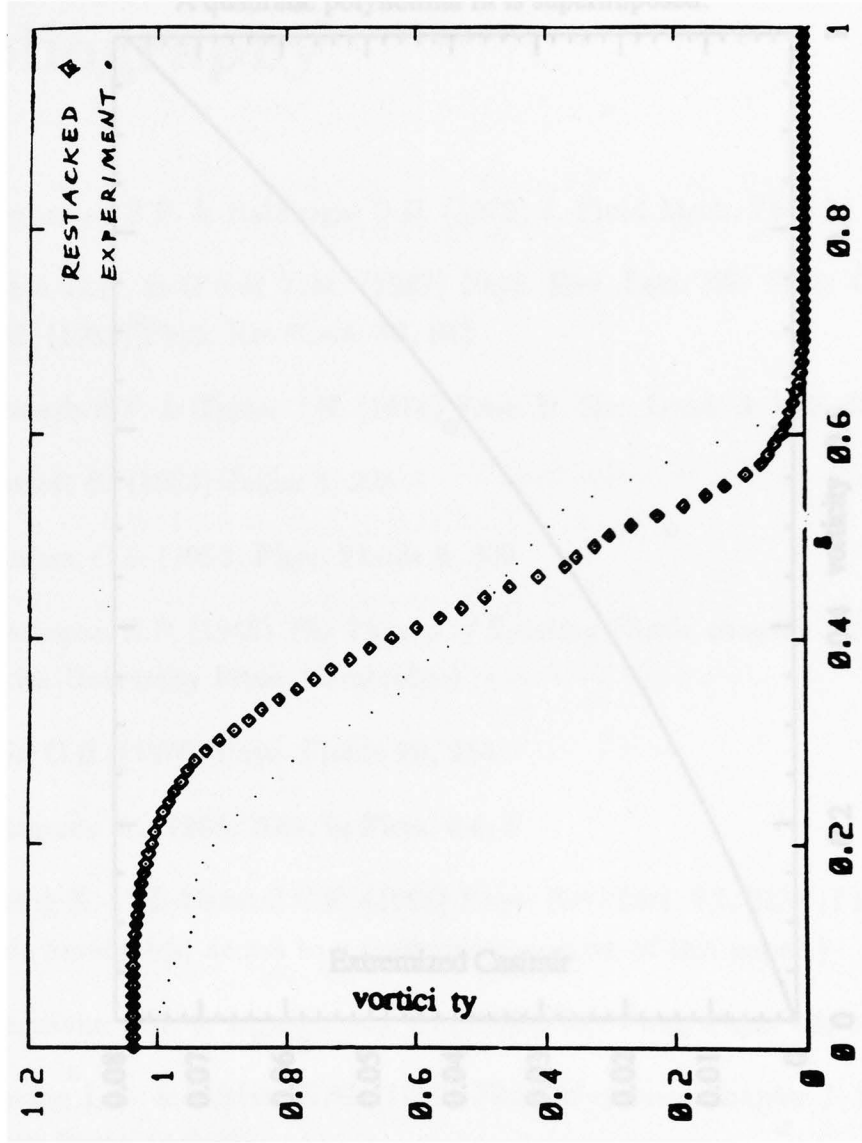

Figure 4.2
The extremized Casimir is plotted versus the vorticity. The vorticity is measured in units in which the maximum value is 1.
A quadratic polynomial fit is superimposed.

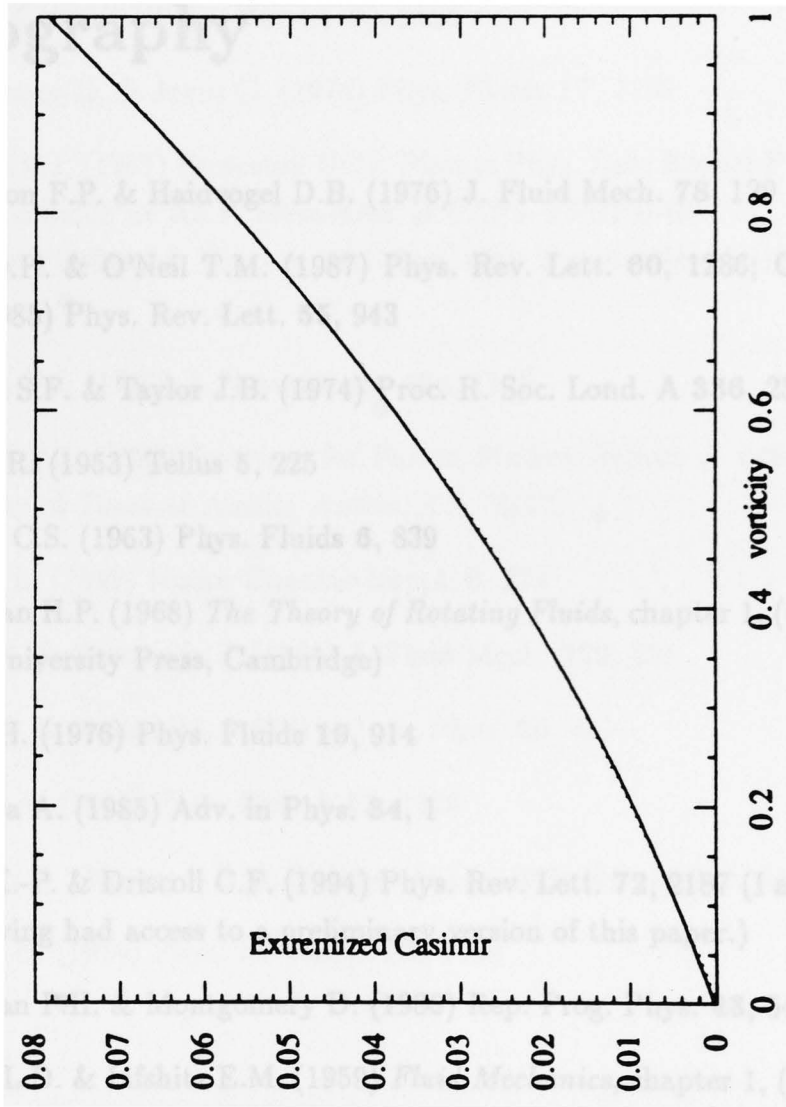

Bibliography

[1] Bretherton F.P. & Haidvogel D.B. (1976) J. Fluid Mech. **78**, 129

[2] Dubin D.H. & O'Neil T.M. (1987) Phys. Rev. Lett. **60**, 1286; O'Neil T.M. (1985) Phys. Rev. Lett. **55**, 943

[3] Edwards S.F. & Taylor J.B. (1974) Proc. R. Soc. Lond. A **336**, 257

[4] Fjortoft R. (1953) Tellus **5**, 225

[5] Gardner C.S. (1963) Phys. Fluids **6**, 839

[6] Greenspan H.P. (1968) *The Theory of Rotating Fluids*, chapter 1, (Cambridge University Press, Cambridge)

[7] Hald O.H. (1976) Phys. Fluids **19**, 914

[8] Hasegawa A. (1985) Adv. in Phys. **34**, 1

[9] Huang X.-P. & Driscoll C.F. (1994) Phys. Rev. Lett. **72**, 2187 (I appreciate having had access to a preliminary version of this paper.)

[10] Kraichnan P.H. & Montgomery D. (1980) Rep. Prog. Phys. **43**, 547

[11] Landau L.D. & Lifshitz E.M. (1959) *Fluid Mechanics*, chapter 1, (Pergamon Press, Oxford)

[12] Leith C.E. (1984) Phys. Fluids **27**, 1388

[13] Lynden-Bell (1967) Mon. Not. R. astr. Soc. **136**, 101

[14] Marcus P. (1988) Nature **331**, 693

[15] Miller J. (1990) Phys. Rev. Lett. **65**, 2137; Miller J., Weichman P.B. & Cross M.C. (1992) Phys. Rev. A **45**, 2328

[16] Montgomery D. & Joyce G. (1974) Phys. Fluids **17**, 1139

[17] Morrison P.J. (1981) Princeton Univ. Plasma Phys. Lab. Report PPPL–1783, (Available as A.I.P. Document # PAPS–PFBPE–04–771, A.I.P. Auxiliary Publication Service, 335 East 45th Street, New York, NY 10017.)

[18] Morrison P.J. (1987) Z. Naturforsch. **42a**, 1115

[19] Morrison P.J. (1994) Institute for Fusion Studies Report # 640, The University of Texas at Austin, Austin, TX 78712.

[20] Onsager L. (1949) Nuovo Cimento Suppl. **6**, 279

[21] Robert R. & Sommeria J. (1991) J. Fluid Mech. **229**, 291

[22] Rose H.A. & Sulem P.L.(1978) le J. de Phys. **39**, 441

[23] Smith R.A. (1991) Phys. Rev. A **43**, 1126

[24] Sommeria J., Meyers S.D. & Swinney H.L. (1988) Nature **331**, 689

[25] Taylor J.B. (1974) Phys. Rev. Lett. **33**, 1139

The vita has been removed from the digitized version of this document.